Time-Resolved FTIR Difference Spectroscopy for the Study of Photosystem I Particles with Plastoquinone-9 Occupying the A_1 Binding Site†

K. M. Priyangika Bandaranayake, Ruili Wang, T. Wade Johnson,‡ and Gary Hastings*

Department of Physics and Astronomy, Georgia State University, Atlanta, Georgia 30303, and Department of Chemistry, Susquehanna University, Selinsgrove, Pennsylvania 17870

Received June 5, 2006; Revised Manuscript Received August 28, 2006

ABSTRACT: In photosystem I from plants and cyanobacteria a phylloquinone molecule, called A_1, functions as the secondary electron acceptor. In cyanobacteria, genes that encode for proteins involved in phylloquinone biosynthesis can be deleted. Here, we have studied three different gene deletion mutants called *menB*, *menD*, and *menE* mutants. In these mutants, plastoquinone-9 occupies the A_1 binding site. Using time-resolved, step-scan FTIR difference spectroscopy we have produced A_1^-/A_1 FTIR difference spectra for *menB*, *menD*, and *menE* photosystem I particles at 77 K. These difference spectra show that the P700 triplet state (^{3}P700) is formed in a large fraction of the particles. Infrared spectral signatures that are not due to ^{3}P700 are also observed in the spectra and are suggested to be associated with plastoquinone-9 anion formation in a portion of the particles. By subtracting the known ^{3}P700 spectral signatures, we produce an A_1^-/A_1 FTIR difference spectrum for PS I particles with plastoquinone-9 occupying the binding site. This spectrum shows that a band that we have previously assigned to a C⋯O mode of the phylloquinone anion in WT A_1^-/A_1 FTIR DS down-shifts ∼8 cm^{-1} when plastoquinone-9 occupies the A_1 binding site. Using density functional theory type calculations to produce anion minus neutral infrared difference spectra for both phylloquinone and plastoquinone-9, it is shown that such a downshift is reasonable. A_1^-/A_1 FTIR difference spectra, obtained using *menB* mutant photosystem I particles that were incubated in the presence of phylloquinone, are found to be very similar to those obtained using normal WT photosystem I particles. This result indicates that we were able to reincorporate phylloquinone back into the A_1 binding site and that the reincorporated phylloquinone and its immediate protein environment, in both the neutral and anion state, are very similar to that found in wild type photosystem I particles. For the reconstituted *menB* mutant photosystem I particles, no spectral signatures associated with ^{3}P700 are observed, indicating that phylloquinone occupies the A_1 site in all of the reconstituted *menB* particles.

In photosynthetic organisms, light absorption induces the separation of charges across a biological membrane. In this way, solar energy is captured and converted into a membrane electrical potential difference. The charge separation is a multistep process, with electrons being transferred sequentially via a series of cofactors across the membrane. In oxygen-evolving organisms, solar capture and conversion occur in two distinct photosystems called photosystems I and II (PS I and II)[1] (*1*). In both photosystems, quinones are involved in the overall electron-transfer process. However, the function of the quinones in the different systems can be quite varied. In PS I, a phylloquinone (PhQ) species (2-methyl-3-phytyl-1,4 naphthoquinone) acts as the secondary electron acceptor (*2*). This species is called A_1. For A_1 to function as it does in PS I, it has to have some very unique redox properties. In fact, PhQ in PS I has the lowest reduction potential (∼800 mV) of any quinone found in nature. The protein cofactor interactions that are at the heart of the unique PhQ redox properties are, therefore, of considerable interest.

To probe the molecular properties of PhQ in PS I, we have been using time-resolved, step-scan FTIR difference spectroscopy (TRSS FTIR DS). We have produced A_1^-/A_1 FTIR DS for intact PS I particles from *Synecococcus* sp. 7002 (*S7002*) and *Synechocystis* sp. 6803 (*S6803*) at 77 K (*3*). We have also produced A_1^-/A_1 FTIR DS for fully ^{2}H-, ^{15}N-, and ^{13}C-labeled PS I particles (*3*). Comparison of the spectra obtained using labeled and nonlabeled PS I particles allowed us to suggest assignments for many of the bands in the spectra. To further investigate the validity of these assignments, one approach is to obtain spectra for PS I particles in which the PhQ that occupies the binding site has been modified or exchanged. As a first step in this direction, we

† This work was supported by the National Research Initiative of the USDA Cooperative State Research Education and Extension Service Grant number 2004-35318-14889 to G.H.

* Corresponding author. Phone: 404-249-7525. Fax: 404-249-7525. E-mail: ghastings@gsu.edu.

‡ Susquehanna University.

[1] Abbreviations: C═O, carbonyl; C⋯O, semiquinone carbonyl; DFT, density functional theory; DS, difference spectrum, spectra, spectroscopic or spectroscopy; DDS, double difference spectrum; FTIR, Fourier transform infrared; H, hydrogen atom; MQ_4, menaquinone-4; NQ, 1, 4-naphthoquinone; OD, optical density; PS I, photosystem I; PhQ, phylloquinone (2-methyl-3-phytyl-1,4 naphthoquinone, also known as vitamin K_1); PQ_9, plastoquinone-9; *S7002*, *Synechococcus* sp. 7002; *S6803*, *Synechocystis* sp. 6803; TRSS, time-resolved step-scan; WT, wild type.

10.1021/bi0611199 CCC: $33.50
Published on Web 09/30/2006

have produced A_1^-/A_1 FTIR DS using *men*G mutant PS I particles in which a methyl-less PhQ analogue occupies the A_1 binding site (*4*).

One approach to quinone incorporation into the A_1 site in cyanobacterial PS I relies on the deletion of genes that code for enzymes involved in the PhQ biosynthetic pathway. Various mutant cell lines have been produced when various genes were deleted, giving rise to the so-called *men* (men is an abbreviation for menaquinone) mutants (*5*−*8*). In this article, we describe studies on PS I particles from *menB*, *menD*, and *menE* mutant cells. In these mutant cells, PhQ biosynthesis is inhibited and a plastoquinone-9 (PQ_9) molecule is recruited into the A_1 binding site (*5*, *6*). The incorporated PQ_9 is functional as an electron transfer (ET) cofactor, with forward ET from A_1 to F_X still occurring with a lifetime of ∼10−300 μs at RT (*5*, *6*, *9*) .

Many questions remain as to the degree of functionality of the PQ_9 molecule that occupies the binding site, the orientation of PQ_9 in the binding site, and any modifications that may have occurred to the protein environment as a consequence of PQ_9 binding. FTIR difference spectroscopy is a very sensitive probe that can be used to begin to address the above questions, and here, we have produced A_1^-/A_1 FTIR DS using *men* mutant PS I particles in which PQ_9 occupies the A_1 binding site.

Recently, reconstitution of quinones into the A_1 binding site of PS I has been demonstrated using *men*B mutant cells, either by adding quinones to the growth medium of whole cells (*10*) or by incubating *menB* PS I particles in the presence of the quinone of interest (*11*−*13*). These approaches allow one to incorporate a specifically labeled PhQ into the A_1 binding site. Such an approach is of high diagnostic value as far as IR spectroscopy is concerned. In addition, using FTIR DS in combination with the above quinone incorporation strategies allows one to address questions related to the structure of the incorporated quinone and its environment in both the neutral and reduced state. Here, we describe our first experiments heading in this direction, where we have produced A_1^-/A_1 FTIR DS using *men*B mutant PS I particles in which PhQ has been reintroduced back into the A_1 binding site.

MATERIALS AND METHODS

Trimeric PS I particles from *S6803* were prepared as described previously (*14*, *15*). Trimeric PS I particles from *menB*, *D*, and *E* mutant cells from *S6803* were prepared as described (*5*). Photoaccumulated $P700^+/P700$ FTIR DS obtained at room temperature and 77 K were virtually the same for all of the PS I particles studied (data not shown). PhQ was purchased from Aldrich. Ethanol was used as solvent for stock solutions. Quinones were introduced into the A_1 binding site with a reaction center to quinone ratio close to 1:1000. Incubation periods of 8 h to several days (in a refrigerator) were typically used. Following this incubation period, the PS I particles were washed and resuspended in a Tris buffer at pH 8. Photoaccumulated $P700^+/P700$ FTIR DS and time-resolved step-scan FTIR DS were collected as described previously (*3*). Below, we shall refer to the photoaccumulated $P700^+/P700$ FTIR DS and time-resolved step-scan FTIR DS as static and time-resolved spectra, respectively. Density functional theory based calculations were undertaken as described previously, using the B3LYP functional and the 6-31G+(d) basis (*16*).

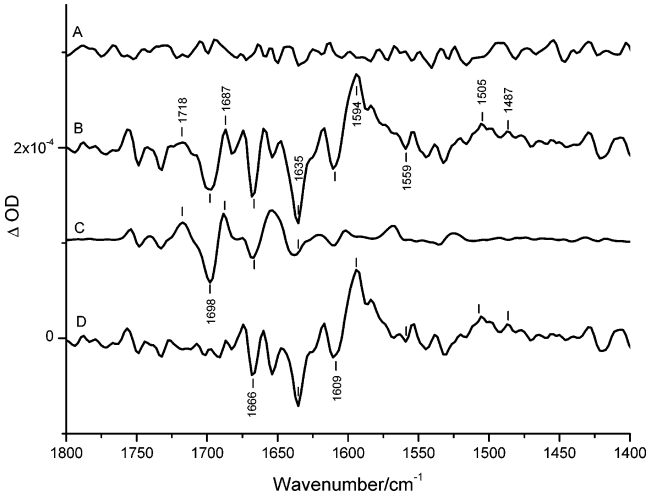

FIGURE 1: Time-resolved (B) and static (C) FTIR DS obtained using *menD* mutant PS I particles from *S6803* at 77 K. The time-resolved spectrum is an average of nine spectra collected in 5 μs increments between 0 and 45 μs, as described previously (*3*). The static spectrum has been scaled by a factor of 7.0. The result of subtracting the static FTIR DS (C) from the time-resolved spectrum B is shown in D. The time-resolved spectrum collected before the laser flash is shown in A and is the average of nine spectra collected in 5 μs increments before the flash. The manipulations used to calculate the spectrum in D are identical to those used to produce the spectra that were previously labeled A_1^-/A_1 FTIR DS (*3*).

RESULTS AND DISCUSSION

Figure 1B shows time-resolved, step-scan FTIR DS obtained following repetitive laser excitation of *menD* mutant PS I particles from *S6803* at 77 K. As described previously, this spectrum is the average of nine spectra, collected in 5 μs increments following the laser flash (*3*).

A time-resolved spectrum collected prior to the laser flash (actually, the average of nine spectra collected in 5 μs increments) is shown in Figure 1A. This spectrum indicates that the noise level in the time-resolved spectra is close to $\pm 1 \times 10^{-5}$ (in optical density (OD) units). Bands in the time-resolved spectrum (Figure 1B) occur at 1635(−), 1594(+) 1609 (−) 1687(+) 1718(+) and 1698(−) cm^{-1}, and are clearly well resolved, given the noise level in the experiment (Figure 1A).

A photoaccumulated $P700^+/P700$ FTIR DS (static spectrum) obtained using *menD* mutant PS I particles at 77 K is shown in Figure 1C. Several bands in the static spectrum in Figure 1C are also observed in the time-resolved spectrum in Figure 1B, in particular, the bands at 1698(−), 1718(+) and 1687(+) cm^{-1}. This indicates that P700 and $P700^+$ contribute to the time-resolved spectrum. By subtracting the static spectrum (Figure 1C) from the time-resolved spectrum (Figure 1B), contributions from P700 and $P700^+$ in the time-resolved spectrum can be eliminated, as previously described (*3*). The results of such a subtraction are shown in Figure 1D. The bands at 1505(+) and 1487(+) cm^{-1} in Figure 1D should be considered suspect because they are below the noise level (Figure 1A). More extensive signal averaging is required to draw any conclusions on these bands. However, any other bands in Figure 1D are well above the noise level.

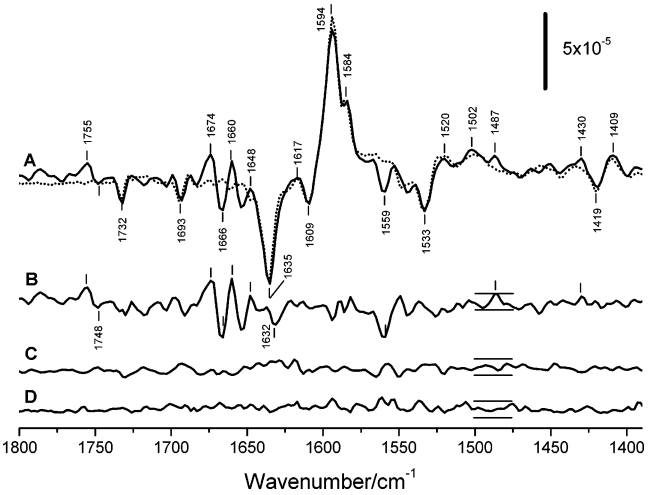

FIGURE 2: (A, solid line) Time-resolved FTIR DS obtained using PS I particles with PQ_9 occupying the A_1 binding site. The spectrum shown is the average of three spectra obtained using *menB*, *D*, and *E* mutant PS I particles and corresponds to the spectrum shown in Figure 1D. The standard deviation in the three averaged spectra is shown in D, and gives a measure of the noise level in the experiments. (A, dotted line) ^{3}P700/P700 FTIR DS collected using PS I particles from *S6803* at 90 K (adapted from ref 17 (*17*), reprinted with permission). (B) Spectrum resulting from the subtraction of the ^{3}P700/P700 FTIR DS (A, dotted line) from the time-resolved spectrum (A, solid line). We call this spectrum an A_1^-/A_1 FTIR DS for PS I particles with PQ_9 occupying the A_1 binding site. (C) Time-resolved FTIR DS collected prior to the laser flash. This spectrum is the average of three spectra obtained using *menB*, *menD*, and *menE* PS I particles. This spectrum is also representative of the noise in the experiments.

We have produced time-resolved and static FTIR DS for *menB*, *menD*, and *menE* PS I particles at 77 K. By subtracting the static P700$^+$/P700 FTIR DS from the time-resolved FTIR DS, a spectrum equivalent to Figure 1D was produced for *menB* and *menE* PS I particles. The spectra obtained for all three mutants are virtually identical to that shown in Figure 1 for *menD*. Figure 2A (solid line) shows the average of the three time-resolved FTIR DS (with contributions from P700$^+$/P700 subtracted). The spectrum in Figure 2A (solid line), therefore, corresponds to the spectrum in Figure 1D, but the noise level is lower because of more extensive signal averaging.

This is clearly seen from the spectra in Figure 2C and D, both of which give an estimate of the noise level in the experiments. The distance between the horizontal bars in Figure 2B indicate the intensity of the band at 1487 cm^{-1}. The same horizontal bars are reproduced in Figure 2C and D and show that the intensity of the 1487 cm^{-1} band in Figure 2B is clearly above the noise level.

In the time-resolved FTIR DS in Figure 2A (solid line), the most prominent feature is a difference band at 1635(−)/1594(+) cm^{-1}. Lower intensity bands are also observed at 1609(−) and 1584(+) cm^{-1}. In addition, a triple feature is clearly observed at 1430(+)/1419(−)/1409(+) cm^{-1}. All of these features are above the noise level (Figure 2C and D) and are characteristic of the triplet state of P700 (^{3}P700) at 77 K (*17*). A digitized version of the ^{3}P700/P700 FTIR DS collected at 90 K is shown as a dotted line in Figure 2A (reproduced with permission). Clearly, all of the bands that are diagnostic of ^{3}P700 are present in our time-resolved spectrum, indicating that ^{3}P700 is formed in a significant fraction of the *men* mutant PS I particles under repetitive laser illumination at 77 K. It is well known that when electron transfer beyond A_0 is blocked, ^{3}P700 can form and decay on a microsecond to millisecond time scale at 77−90 K (*18*). Therefore, in a fraction of the *men*B PS I particles, either the A_1 site is empty or PQ_9 is present in the site but is not oriented in a fashion that is suitable for accepting an electron from A_0^-.

The previously published ^{3}P700/P700 FTIR DS (Figure 2A, dotted line) has not been reproduced by any other group. The ^{3}P700/P700 FTIR DS was obtained using PS I samples that were treated with high concentrations of urea (to remove the terminal acceptors F_A and F_B) in the presence of dithionite, under illumination at 90 K (*17*). Furthermore, a contribution from P700$^+$/P700 was also subtracted. Given these conditions, the ^{3}P700/P700 FTIR DS could justifiably be viewed with skepticism. However, the fact that we obtain a time-resolved spectrum displaying features that are virtually identical to those found in the ^{3}P700/P700 FTIR DS supports the validity of the previously published spectrum. The ^{3}P700/P700 FTIR DS was obtained at 90 K, whereas the time-resolved spectrum in Figure 2A was obtained at 77 K. The fact that the two spectra in Figure 2A display many similar features indicates that the 13 K temperature difference is irrelevant. Also, P700$^+$/P700 FTIR DS collected at 77 and 90 K are identical (data not shown), again indicating that the 13 K temperature difference is irrelevant.

Several bands are present in the time-resolved FTIR DS in Figure 2A (solid line) that are absent in the ^{3}P700/P700 FTIR DS (Figure 2A, dotted line). To more easily analyze these bands, we have subtracted the ^{3}P700/P700 FTIR DS from the time-resolved FTIR DS. The resultant spectrum is shown in Figure 2B. Bands are observed at 1755(+), 1748(−), 1674(+), 1666(−), 1660(+), 1654(−), 1632(−), 1559(−), 1549(+), and 1487(+) cm^{-1}. Our hypothesis is that these bands are associated with PQ_9 reduction in the *men* mutant PS I particles. We, therefore, call this spectrum the PQ_9 A_1^-/A_1 FTIR DS. The picture emerging from the time-resolved FTIR DS in Figure 2 is that PQ_9 is functional only in a fraction of the PQ_9-containing PS I particles. In the portion of reaction centers in which PQ_9 is not functional or missing, the primary radical pair state P700$^+$ A_0^- recombines to form the triplet state.

Our hypothesis is that ^{3}P700 and P700$^+$ PQ_9^- both form upon laser illumination of *menB*, *D*, or *E* mutant PS I particles at 77 K. Given this, it is important to investigate if the decay of the two different states can be distinguished. Figure 3 shows absorption changes at 1699, 1635, 1594, and 1487 cm^{-1} observed following the excitation of PQ_9-containing *men* mutant PS I particles at 77 K. Following the excitation of PQ_9-containing PS I, a bleaching is observed at 1635 cm^{-1} and an absorption increase at 1594 cm^{-1}. Such changes are indicative of ^{3}P700 formation. The absorption changes at both 1635 and 1594 cm^{-1} decay with a time constant of 208 μs, leaving a residual component that decays on timescales longer than 1 ms. Thus, in PQ_9-containing PS I, ^{3}P700 forms and then decays with a time constant of 208 μs. Residual, longer-lived absorption changes are due to the P700$^+$ PQ_9^- (see below) .

Following excitation of PQ_9-containing PS I, a bleaching is observed at 1699 cm^{-1} that hardly decays in 1 ms. This is very different from the kinetics at 1635 and 1594 cm^{-1}.

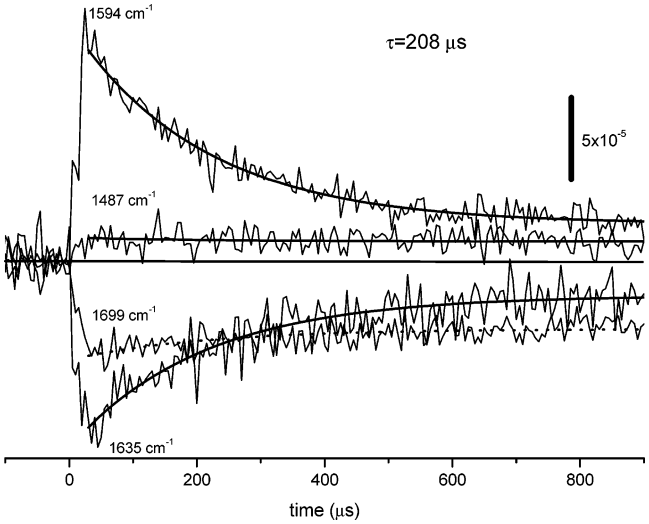

FIGURE 3: Kinetics of the absorption changes observed at 1699, 1635, 1594, and 1487 cm^{-1}, obtained following 532 nm laser excitation of PQ_9-containing PS I particles from *S6803*. Data was collected in 5 μs increments. The four kinetic traces were fitted simultaneously to a single decaying exponential component plus a constant (nondecaying) component. The fitted functions shown (thick smooth lines) are characterized by a time constant of 208 μs. Each kinetic is the average of kinetics obtained using *menB, D,* and *E mutant* PS I particles.

Absorption changes at 1699 cm^{-1} are due to $P700^+$ formation. Therefore, the 1699 cm^{-1} kinetic indicates $P700^+$ formation with little decay of this state in 1 ms. The 1699 cm^{-1} kinetic, therefore, supports the idea that $P700^+$ PQ_9^- forms upon light excitation and then decays on a millisecond time scale. The time constant governing the decay of the $P700^+$ PQ_9^- state was not established in the experiments reported here. Interestingly, a light induced absorption increase is observed at 1487 cm^{-1}, which does not appear to decay in 1 ms. This suggests that the absorption increase at 1487 cm^{-1} is associated with the $P700^+$ PQ_9^- state rather than the $^3P700$ state. Below, we present evidence supporting the idea that the absorption increase at 1487 cm^{-1} is due to PQ_9^- formation.

In *menB* mutants with PQ_9 occupying the A_1 binding site, it has been shown that the spin-polarized transient EPR spectrum for the PQ_9 anion radical can be obtained without features that are characteristic of the triplet state (*10*). The transient EPR experiments are undertaken in a somewhat similar manner to the time-resolved FTIR experiments, and the origin of the differing results are not clear. In the time-resolved FTIR experiments, samples are illuminated with laser flashes at 10 Hz for ~20 h. Thus, over many laser flashes, forward ET may be inhibited in some of the reaction centers (with PQ_9 in the binding site). We are currently investigating this possibility.

Previously, Johnson et al. (*10*) showed that X- and Q-band spin-polarized transient EPR spectra of PS I from *menB* mutants with menaquinone-4 (MQ_4) occupying the A_1 site are virtually identical to the spectra obtained using WT PS I particles. MQ_4 was added to the growth medium and was taken up by the living cells. It has also been shown that by incubating *menB* PS I particles in the presence of PhQ, PhQ will displace PQ_9 in the A_1 binding site (*11*) and that the EPR characteristics of the reincorporated PhQ are very similar to native PhQ in PS I (*11*). Thus, in the *menB* PS I particles, the reincorporated PhQ anion radical that is EPR active is oriented and positioned in a manner that is very similar to native PhQ^- in WT PS I particles. The EPR measurements do not directly address how the protein environment around the incorporated pigment is modified, nor do they address details associated with the incorporated pigment in the ground state. FTIR DS is a sensitive probe of both the ground state and the radical anion state. In addition, bands in the A_1^-/A_1 FTIR DS are very sensitive to the protein environment around the A_1 site. Therefore, FTIR DS provides a means to very stringently probe both the neutral and anion states of PhQ and its environment in *menB* PS I particles in comparison to PhQ in WT PS I particles.

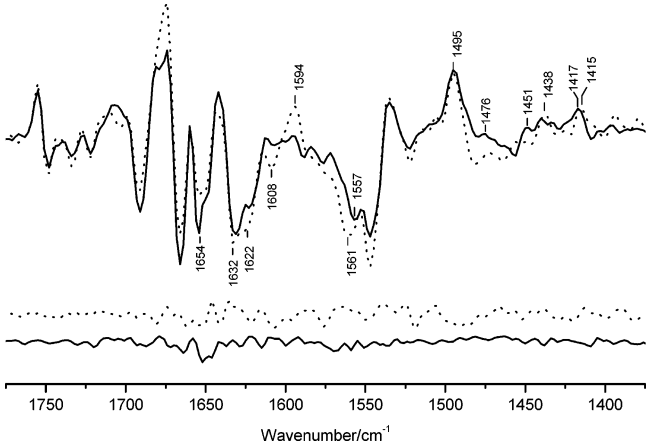

FIGURE 4: Comparison of A_1^-/A_1 FTIR DS obtained using *menB* PS I particles reconstituted with PhQ (solid line) or WT PS I particles (dotted). Corresponding time-resolved FTIR DS collected prior to the laser flash, which are representative of the noise level in the experiments, are also shown.

Figure 4 compares A_1^-/A_1 FTIR DS obtained using *menB* PS I particles reconstituted with PhQ and that obtained using WT PS I particles. There are some small changes in band intensities, but band frequency shifts are negligible. Thus, the FTIR data in Figure 4 indicate that PhQ can be reconstituted back into PS I particles in the same orientation as that in WT PS I (however, the actual orientation of PhQ in the A_1 site cannot be quantitatively determined from the FTIR spectra) and that there is little alteration in the protein binding site for both the neutral and anion states.

In the A_1^-/A_1 FTIR DS obtained using WT PS I particles, a derivative feature appears at 1608(−)/1594(+) cm^{-1} (Figure 4). This feature is absent in the spectrum for PhQ reconstituted PS I particles. This feature is reminiscent of a derivative band at the same frequency in the $^3P700/P700$ FTIR DS (Figure 2A, dotted line). However, no other band that is indicative of $^3P700$ can be distinguished in the A_1^-/A_1 FTIR DS obtained using WT PS I particles. This might occur because the other triplet bands are below the noise level (shown in Figure 4) or are masked by more intense radical bands (as may be the case for the 1635(−) cm^{-1} triplet band). At present, we cannot, therefore, rule out the possibility that some small amount of $^3P700$ triplet state is formed under our experimental conditions in WT PS I particles at 77 K. We also cannot rule out the possibility that the differences in the spectra in Figure 4, in the 1610−1540 cm^{-1} region, are associated with changes in protein modes.

In A_1^-/A_1 FTIR DS obtained using intact cyanobacterial PS I particles (Figure 4, dotted line), we have associated the positive band at 1495(+) cm^{-1} with a C⋯O mode of PhQ^- (*4*). A band is found at exactly the same frequency in PhQ reconstituted *menB* PS I particles (Figure 4, solid line). This suggests that the C⋯O mode of the introduced PhQ in the anion state is unaltered. This further suggests little alteration of the electronic structure of the NQ head group of PhQ^- in *menB* PS I particles. Given this, it appears very likely that the C═O modes of neutral PhQ should also not be altered in the FTIR DS.

Previously, we suggested that a negative band at 1654 (−) cm^{-1} could be due to a C═O mode of neutral PhQ in the A_1 site that is free from H-bonding (*3*). A band at 1654(−) cm^{-1} is also observed in PhQ reconstituted *men*B PS I particles. In fact, the 1654(−) cm^{-1} band appears to have greater intensity in the mutant spectrum. However, this may be somewhat related to the choice of an appropriate scaling factor.

We have also suggested that a negative band at 1608 (−) cm^{-1} could be due to an H-bonded C═O mode of neutral PhQ in the A_1 site (*3*). No band is observed at 1608(−) cm^{-1} in the A_1^-/A_1 FTIR DS of *men*B mutant PS I particles with reconstituted PhQ. There are at least three possible explanations for this. (1) The origin of the 1608 cm^{-1} band proposed previously is incorrect. (2) The H-bonding nature of the C═O mode of the introduced PhQ is altered. (3) The 1608 (−) cm^{-1} band is obscured because of changing protein modes. The spectra in Figure 4 do suggest that there are some changes in protein modes in PhQ reconstituted *menB* PS I. For example, the negative band at 1561 cm^{-1} for WT PS I is likely associated with amide II absorption bands. This band appears to downshift to 1557 cm^{-1} in PhQ reconstituted *menB* PS I.

Although there are some differences in the spectra in Figure 4, the key feature for this article is that a positive band is found at 1495 cm^{-1} in both spectra in Figure 4. In A_1^-/A_1 FTIR DS obtained using WT PS I, this positive band is due to a C⋯O mode of PhQ^- (*4*).

Because we have acquired an A_1^-/A_1 FTIR DS obtained using *menB* mutant PS I particles with PhQ occupying the A_1 binding site (Figure 4, solid line), we can now ask how this spectrum compares to A_1^-/A_1 FTIR DS obtained using *menB* mutant PS I particles with PQ_9 occupying the A_1 site.

Figure 5 compares A_1^-/A_1 FTIR DS obtained using *menB* mutant PS I particles with PhQ (A) or PQ_9 (B) occupying the A_1 binding site. To closely compare the two spectra, the PQ_9 A_1^-/A_1 FTIR DS is also shown as dotted line in Figure 5A. The spectra were scaled so that difference bands in the 1680−1660 cm^{-1} region have similar intensity.

The spectra in Figure 5 show some common features. In particular, a band is found at 1755(+)/1748(−) cm^{-1} in both spectra. Previously, we assigned this band to the 13[3] ester C═O mode of the A_0 chlorophyll-*a*, which became visible because of an electrochromic effect caused by the negative charge on the A_1 pigment. The observation of the same difference band in both spectra in Figure 5 suggests that the same type of electrochromic effect occurs when either PhQ or PQ_9 occupies the A_1 site. This is likely to be true only if the quinone head groups are similarly oriented, that is, the C═O groups of both quinones point in the same direction in the A_1 site.

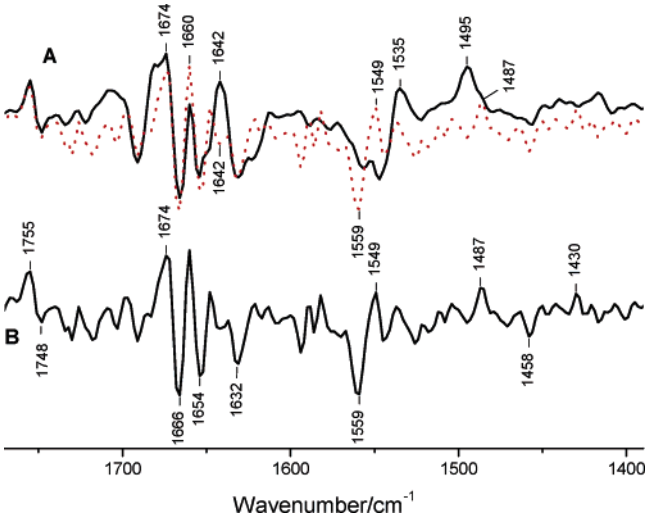

FIGURE 5: (A, solid line) A_1^-/A_1 FTIR DS obtained using *menB* PS I particles in which PhQ has been reconstituted back into the A_1 binding site. This spectrum is also shown in Figure 4 (solid line). (B) A_1^-/A_1 FTIR DS obtained using *menB* mutant PS I particles in which PQ_9 occupies the A_1 binding site. This spectrum is shown as a dotted line in A and is also presented in Figure 2B.

In Figure 5B, a positive band is observed at 1487 cm^{-1}. The 1487 cm^{-1} kinetic trace in Figure 3 as well as the estimates of the noise level in Figure 2C and D, indicates that the 1487 cm^{-1} band is well resolved. It is possible that the 1487 cm^{-1} band found in the PQ_9 A_1^-/A_1 FTIR DS corresponds to the 1495 cm^{-1} band found in the PhQ A_1^-/A_1 FTIR DS spectrum. If this is the case, then the 1487 cm^{-1} band is associated with a C⋯O mode of PQ_9^-. The suggestion is, therefore, that the C⋯O mode of PQ_9^- in A_1 binding is ∼8 cm^{-1} lower than the C⋯O mode of PhQ^-. To test if this is reasonable, we have undertaken density functional theory (DFT) based harmonic normal mode vibrational frequency calculations for the neutral and reduced forms of the PhQ and PQ_9 models shown in Figure 6A and B, respectively. The phytyl chain, truncated as shown in Figure 6, has no impact on the calculated vibrational frequencies (*16*). Figure 7A shows calculated anion minus neutral FTIR DS for the PhQ (dotted line) and PQ_9 (solid line) models shown in Figure 6. The highest intensity mode frequencies and their assignments are listed in Table 1.

Calculated vibrational frequencies are generally higher than experimentally observed frequencies, with no single scaling factor being directly applicable (*19*). In the DFT calculations presented here, we are primarily interested in vibrational frequency differences, and we have shown that these frequency differences can be accurately calculated without scaling (*16*). We have, therefore, chosen not to change the frequency scale for the spectra in Figure 7.[2]

Notice also that the experimental spectra in Figure 5 contain contributions from protein modes, whereas the calculated spectra in Figure 7 do not. This is why the spectra in Figures 5 and 7 look different.

The PhQ model in Figure 6A contains 31 atoms. There are, therefore, 87 normal modes of vibration for this molecule. Most of these modes are of low intensity and are

[2] Previously, we indicated that if desired, a frequency scaling factor of 0.965 is appropriate for frequencies in the 1800−1600 cm^{-1} range and 0.989 for frequencies near 1300 cm^{-1} (*16*).

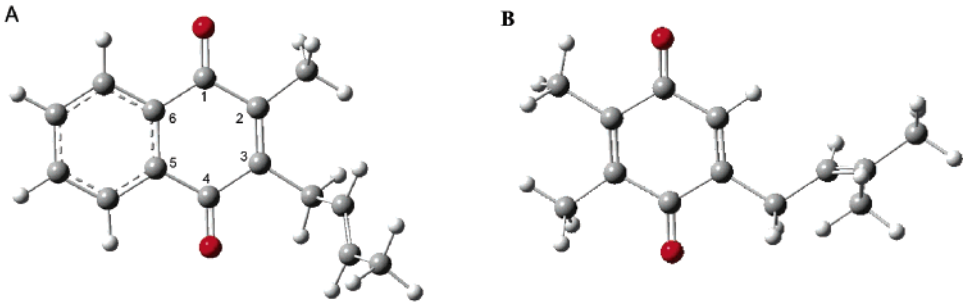

FIGURE 6: Structure of the (A) PhQ and (B) PQ_9 models used in DFT calculations. The structures were optimized using the B3LYP/6-31+G(d) method. In A, part of the IUPAC numbering scheme is also shown. The PhQ model is the same as that used previously (*16*).

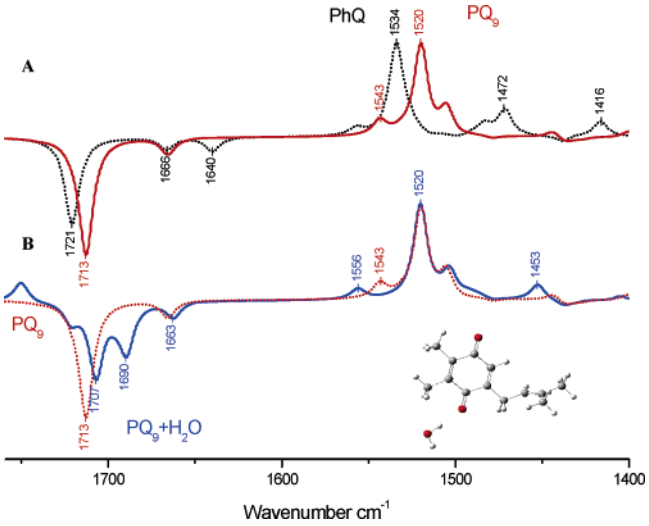

FIGURE 7: (A) Calculated IR difference spectra (anion minus neutral) for the PhQ (dotted line) and PQ_9 (solid line) models shown in Figure 6A and B, respectively. The PhQ spectrum has been presented previously (*16*). The spectrum calculated for PQ_9 in the presence of a water molecule (model shown in the inset) close to the C_4═O is also shown (B, solid line). The PQ_9 spectrum from part A is also shown as a dotted line in B to aid in comparison.

not observable in Figure 7A, and they will not be observable in experimental FTIR DS. The modes that give rise to the prominent bands in Figure 7A are the ones most likely to be observable experimentally, and we will consider only these modes here.

For PhQ, the negative band at 1721 cm^{-1} (1660 cm^{-1} after scaling) is due to the asymmetric vibration of both carbonyl groups of neutral PhQ. The asymmetric vibration of both carbonyl groups of PhQ^- occurs at 1534 cm^{-1} (*4*). For PQ_9/PQ_9^-, the corresponding modes occur at 1713 and 1520 cm^{-1}, respectively, that is, the calculations predict that the C═O/C⋯O modes of PQ_9/PQ_9^- are 8 and 14 cm^{-1} lower than the corresponding modes of PhQ and PhQ^-, respectively.

Our hypothesis, derived from the data in Figure 5, is that the C⋯O mode of PQ_9^- is 8 cm^{-1} lower than the corresponding mode for PhQ^-. Thus, the calculation outlined in Figure 7 over estimates the downshift but correctly predicts the trend that the C⋯O mode of PQ_9^- is at a lower frequency than that of the same mode of PhQ^-. The calculated result, therefore, provides some support for the idea that the positive band at 1487(+) cm^{-1} in the PQ_9 A_1^-/A_1 FTIR DS is due to a C⋯O mode of PQ_9^-, which is downshifted 8 cm^{-1} relative to the corresponding mode for PhQ^-.

From studies of PQ_9 in ethanol, it has been suggested that a band at 1471 cm^{-1} is due to a C⋯O vibration (*20*). For PhQ^- in CH_2Cl_2, the asymmetric C⋯O mode was found to occur at 1488 cm^{-1} upon one electron reduction (*21*). Experimentally then, the asymmetric C⋯O mode of PhQ^- is 17 cm^{-1} higher than that found for the corresponding mode in PQ_9^-. The different solvents used in these two studies may account for some of this difference. Therefore, the calculations outlined in Figure 7A appear to predict the correct trends observed in the experimental data for PhQ^- and PQ_9^- in solvent.

Notice that the bands that we associate with C⋯O vibrations of PhQ^- and PQ_9^- in the A_1 binding site have higher frequencies than those associated with the isolated pigments in solution (1495/1487 cm^{-1} for PhQ^-/PQ_9^- in the A_1 site versus 1488/1471 cm^{-1} for PhQ^-/PQ_9^- in solution, respectively). The same trend is also observed for Q_A^-/Q_A FTIR DS obtained using PS II particles (Q_A is also a PQ_9 molecule), where the main C⋯O vibration occurs at 1478 cm^{-1} (*22*) versus 1471 cm^{-1} for PQ_9^- in ethanol (*20*).

The negative band at 1721(−) cm^{-1} in Figure 7A is due to the asymmetric stretching of both C═O modes of neutral PhQ. Similarly, the negative band at 1713 cm^{-1} in Figure 7A (dotted line) is due to the asymmetric stretching of both C═O modes of neutral PQ_9. Therefore, the calculations indicate that the C═O mode of neutral PQ_9 will also be at a lower frequency (8 cm^{-1}) than that for PhQ. For PQ_9 in ethanol, the C═O asymmetric stretching vibration occurs at 1653 cm^{-1} (*20*, *22*), whereas for neat PhQ, it occurs at 1661 cm^{-1} (*23*). Again, the calculations agree very well with the experimental FTIR spectra for PhQ and PQ_9 in solvent.

It is not entirely clear how to interpret the bands in the C═O region of the PQ_9 A_1^-/A_1 FTIR DS in Figure 5. In this respect, the calculations can be a useful guide. For example, in A_1^-/A_1 FTIR DS obtained using WT PS I, it has been suggested that a C═O mode of neutral PhQ contributes to a negative absorption change near 1654 cm^{-1}. If this is correct, then the calculations outlined in Figure 7 suggest that a negative band may be found near 1646 cm^{-1} in A_1^-/A_1 FTIR DS obtained using PQ_9-containing *menB* mutant PS I. In fact, a negative band is observed at 1642-(−) cm^{-1} in the PQ_9 A_1^-/A_1 FTIR DS (Figure 5), whereas a positive band is found at the same frequency in the PhQ A_1^-/A_1 FTIR DS. Thus, the calculations suggest that the 1642 cm^{-1} band in A_1^-/A_1 FTIR DS, obtained using *menB* mutant PS I, could be due to a C═O mode of PQ_9. Notice, however, that the 1642 cm^{-1} band has an intensity that is close to the noise level (Figure 2). The above hypothesis should, therefore, be viewed with some skepticism.

Table 1: Approximate Mode Frequencies (in cm^{-1}) and Intensities (in km/mol) for PQ_9 and PQ_9^- Calculated for the Model Molecules Shown in Figure 6A and B[a]

mode	PQ	mode	PQ+H_2O (C_4=O)
ν(C=C, C=O)$_s$	1721 (15)	ν(C=C, C=O)$_s$[b], δ(C−H)	1721 (78)
ν(C=O)$_{as}$	1713 (447)	ν(C=O)$_{as}$, δ(H_2O)	1707(313)
		ν(C=O)$_{as}$[c], δ(H_2O)	1689(205)
ν(C=C)$_{as}$	1665 (64)	ν(C=C)$_{as}$	1662(68)
mode	PQ^-	mode	PQ^-+H_2O (C_4=O)
		δ(H_2O)	1749(84)
ν(C=C)$_{as}$, δ(C−H)	1543 (56)	ν(C=C)$_{as}$, δ(C−H)	1556(44)
ν(C=O)$_{as}$, δ(C−H)	1519 (365)	ν(C=O)$_{as}$, $(CH_3)_{C-H\ twist}$	1520(372)
$(CH_3)_{C-H\ twist}$	1505 (102)	ν(C_1=O), $(CH_3)_{C-H\ twist}$	1519(48)
		ν(C=O)$_s$, δ(C−H)	1503(121)

[a] Also listed are the mode frequencies and intensities for PQ9 and PQ9$^-$ in the presence of a water molecule near the C_4=O group (Figure 7, inset). Abbreviations: *s*; symmetric, *as*; asymmetric. [b] More C_1=O than C_4=O. [c] Mainly C_4=O.

It is possible, even likely, that the PQ_9 molecules active in the A_1 site in *menB* mutant PS I could be H bonded, as is the case for PhQ in WT PS I. The orientation of the PQ_9 head group in the A_1 site is thought to be the same for the quinone ring of PhQ, with the C_4=O group involved in H bonding to a leucine residue. In an attempt to more accurately model this possible interaction for the PQ_9 molecule occupying the A_1 binding site in *menB* mutant PS I, we have calculated the vibrational properties of PQ_9 and PQ_9^- in the presence of a water molecule, which is H bonded to the C_4=O of PQ_9 (Figure 7, inset). The water H atom is 1.76 Å from the carbonyl oxygen, whereas the oxygen atoms are separated by 2.73 Å. The calculated difference spectrum for the PQ_9 + H_2O model is shown in Figure 7B, and the most relevant mode frequencies and their intensities are listed in Table 1. Calculated spectra for PhQ with the C_4=O H bonded to a water molecule have been presented previously (*4*).

For neutral PQ_9 in the presence of one water molecule (near the C_4=O), we find that the asymmetric C=C mode frequency decreases by 3 cm^{-1} and is hardly changed in intensity. For the anion state, however, the asymmetric C=C vibration increases in frequency by 13 cm^{-1} and decreases in intensity by ∼22%. These observations are similar to those found for neutral and reduced PhQs in the presence of a water molecule (*4*).

For neutral PQ_9, the presence of a water molecule causes a 6 cm^{-1} downshift of the asymmetric C=O vibration (from 1713 to 1707 cm^{-1}) and a considerable decrease in intensity of the mode. The water molecule actually leads to a splitting of the asymmetric C=O vibration, with a second asymmetric C=O mode appearing at 1689 cm^{-1}. Note, however, that the 1689 cm^{-1} mode is not a pure asymmetric vibration of both C=O groups because the C_4=O stretching has a much larger amplitude than the C_1=O stretching.

For PQ_9^-, the asymmetric C⋯O mode at 1519 cm^{-1} splits into two modes at 1520 and 1503 cm^{-1} when a water molecule is added. The mode at 1520 cm^{-1} carries ∼75% of the intensity. As far as the IR difference spectra are concerned, the presence of a water molecule does not change the fact that an intense band due to the asymmetric C⋯O mode still appears at 1520 cm^{-1} (compare the lower two spectra in Figure 7B). This frequency is still considerably lower than that found for the same mode of PhQ in the presence or absence of a water molecule (1534−1536 cm^{-1}). Therefore, independent of the H-bonding status of the C_4=O group, the C⋯O vibration of PQ_9^- is calculated to be ∼14 cm^{-1} lower in frequency than that of the same mode of PhQ^-.

CONCLUSIONS

Under our experimental conditions (temperature = 77 K and many thousands of laser flashes at 532 nm), we find that PQ_9 is functional as an ET cofactor in only a fraction of the *menB* mutant PS I particles. In the fraction where PQ_9 is not functional (or perhaps not even present), we find, as one might expect, that ^{3}P700 is formed. We find that ^{3}P700 decays in ∼208 μs, whereas $P700^+PQ_9^-$ decays on a time scale much greater than 1 ms. In the fraction where PQ_9 is functional as an electron-transfer cofactor, we are able to generate an A_1^-/A_1 FTIR DS. A band that we have previously suggested to be associated with a C⋯O mode of PhQ^- appears to downshift ∼8 cm^{-1} when PQ_9 occupies the binding site. Vibrational mode frequency calculations for PhQ^- and PQ_9^- in the gas phase show that a downshift of 14 cm^{-1} may be expected. Thus, the calculations predict the observed trend but not the magnitude of the downshift. Such a downshift does, however, agree well with experiments undertaken on PhQ and PQ_9 in solvent.

Using *menB* mutant PS I particles that have been incubated in the presence of PhQ, we show that an A_1^-/A_1 FTIR DS is obtained, which is very similar to that obtained using WT PS I particles (that have PhQ in the A_1 site). Thus, the added PhQ displaces PQ_9. For the *menB* particles reconstituted with PhQ, no sign of spectral signatures associated with ^{3}P700 are observed in the A_1^-/A_1 FTIR DS, demonstrating that PhQ occupies the A_1 binding site in all of the *menB* PS I particles.

REFERENCES

1. Barber, J. (1992) *The Photosystems : Structure, Function, and Molecular Biology*, Vol. 11, Elsevier Science Publishers, Amsterdam and New York.
2. Golbeck, J. H., and Bryant, D. (1991) *Photosystem I: Current Topics in Bioenergetics*, pp 83−175, Academic Press, New York.
3. Sivakumar, V., Wang, R., and Hastings, G. (2005) A_1 reduction in intact cyanobacterial photosystem I particles studied by time-resolved step-scan Fourier transform infrared difference spectroscopy and isotope labeling, *Biochemistry 44*, 1880−1893.
4. Bandaranayake, K. M., Wang, R., and Hastings, G. (2006) Modification of the phylloquinone in the A_1 binding site in photosystem I studied using time-resolved FTIR difference spectroscopy and density functional theory, *Biochemistry 45*, 4121−4127.

5. Johnson, T. W., Shen, G., Zybailov, B., Kolling, D., Reategui, R., Beauparlant, S., Vassiliev, I. R., Bryant, D. A., Jones, A. D., Golbeck, J. H., and Chitnis, P. R. (2000) Recruitment of a foreign quinone into the A_1 site of photosystem I. I. Genetic and physiological characterization of phylloquinone biosynthetic pathway mutants in Synechocystis sp. pcc 6803, *J. Biol. Chem. 275*, 8523−8530.
6. Zybailov, B., van der Est, A., Zech, S. G., Teutloff, C., Johnson, T. W., Shen, G., Bittl, R., Stehlik, D., Chitnis, P. R., and Golbeck, J. H. (2000) Recruitment of a foreign quinone into the A(1) site of photosystem I. II. Structural and functional characterization of phylloquinone biosynthetic pathway mutants by electron paramagnetic resonance and electron-nuclear double resonance spectroscopy, *J. Biol. Chem. 275*, 8531−8539.
7. Johnson, T. W., Naithani, S., Stewart, C., Zybailov, B., Jones, A. D., Golbeck, J. H., and Chitnis, P. R. (2003) The menD and menE homologs code for 2-succinyl-6-hydroxyl-2,4-cyclohexadiene-1-carboxylate synthase and O-succinylbenzoic acid-CoA synthase in the phylloquinone biosynthetic pathway of Synechocystis sp PCC 6803, *Biochim. Biophys. Acta 1557*, 67−76.
8. Sakuragi, Y., Zybailov, B., Shen, G. Z., Jones, A. D., Chitnis, P. R., van der Est, A., Bittl, R., Zech, S., Stehlik, D., Golbeck, J. H., and Bryant, D. A. (2002) Insertional inactivation of the *menG* gene, encoding 2-phytyl-1, 4-naphthoquinone methyltransferase of *Synechocystis* sp. PCC 6803, results in the incorporation of 2-phytyl-1,4-naphthoquinone into the A(1) site and alteration of the equilibrium constant between A(1) and F-x in photosystem I, *Biochemistry 41*, 394−405.
9. Semenov, A. Y., Vassiliev, I. R., van Der Estqq, A., Mamedov, M. D., Zybailov, B., Shen, G., Stehlik, D., Diner, B. A., Chitnis, P. R., and Golbeck, J. H. (2000) Recruitment of a foreign quinone into the A_1 site of photosystem I. Altered kinetics of electron transfer in phylloquinone biosynthetic pathway mutants studied by time-resolved optical, EPR, and electrometric techniques, *J. Biol. Chem. 275*, 23429−23438.
10. Johnson, T. W., Zybailov, B., Jones, A. D., Bittl, R., Zech, S., Stehlik, D., Golbeck, J. H., and Chitnis, P. R. (2001) Recruitment of a foreign quinone into the A_1 site of photosystem I. In vivo replacement of plastoquinone-9 by media-supplemented naphthoquinones in phylloquinone biosynthetic pathway mutants of *Synechocystis* sp., *PCC 6803*, *J. Biol. Chem. 276*, 39512−39521.
11. Pushkar, Y., Golbeck, J., Stehlik, D., and Zimmermann, H. (2004) Asymmetric hydrogen-bonding of the quinone cofactor in photosystem I probed by ^{13}C labeled naphthoquinones, *J. Phys. Chem. B 108*, 9439−9448.
12. Pushkar, Y., Zech, S., Stehlik, D., Brown, S., van der Est, A., and Zimmermann, H. (2002) Orientation and protein-cofactor interactions of monosubstituted n-alkyl naphthoquinones in the A_1 binding site of photosystem I, *J. Phys. Chem. B 106*, 12052−12058.
13. Pushkar, Y. N. (2005) Transient and pulsed EPR study of O-17-substituted methyl-naphthoquinone as radical anion in the A(1) binding site of photosystem I and in frozen solution, *Appl. Magn. Reson. 28*, 195.
14. Hastings, G., Reed, L., Lin, S., and Blankenship, R. (1995) Excited state dynamics in photosystem I: effects of detergent and excitation wavelength, *Biophys. J. 69*, 2044−2055.
15. Hastings, G., Hoshina, S., Webber, A., and Blankenship, R. (1995) Universality of energy and electron transfer processes in photosystem I, *Biochemistry 34*, 15512−15522.
16. Bandaranayake, K., Sivakumar, V., Wang, R., and Hastings, G. (2006) Modeling the A_1 binding site in photosystem I. Density functional theory for the calculation of "anion−neutral" FTIR difference spectra of phylloquinone, *Vib. Spectrosc.*, in press.
17. Breton, J., Nabedryk, E., and Leibl, W. (1999) FTIR study of the primary electron donor of photosystem I (P700) revealing delocalization of the charge in P700(+) and localization of the triplet character in (3)P700, *Biochemistry 38*, 11585−11592.
18. Brettel, K. (1997) Electron transfer and arrangement of the redox cofactors in photosystem I, *Biochim. Biophys. Acta 1318*, 322−373.
19. Rauhut, G., and Pulay, P. (1995) Transferable scaling factors for density-functional derived vibrational force-fields, *J. Phys. Chem. 99*, 3093−3100.
20. Razeghifard, M. R., Kim, S., Patzlaff, J. S., Hutchison, R. S., Krick, T., Ayala, I., Steenhuis, J. J., Boesch, S. E., Wheeler, R. A., and Barry, B. A. (1999) In vivo, in vitro, and calculated vibrational spectra of plastoquinone and the plastosemiquinone anion radical, *J. Phys. Chem. B 103*, 9790−9800.
21. Bauscher, M., and Mantele, W. (1992) Electrochemical and infrared-spectroscopic characterization of redox reactions of p-quinones, *J. Phys. Chem. 96*, 11101−11108.
22. Berthomieu, C., Nabedryk, E., Mantele, W., and Breton, J. (1990) Characterization by FTIR spectroscopy of the photoreduction of the primary quinone acceptor QA in photosystem II, *FEBS Lett. 269*, 363.
23. Hastings, G., and Sivakumar, V. (2001) A Fourier transform infrared absorption difference spectrum associated with the reduction of A1 in photosystem I: Are both phylloquinones involved in electron transfer? *Biochemistry 40*, 3681−3689.

BI0611199